Biochemistry and Biophysics Reports 42 (2025) 101971

Contents lists available at ScienceDirect

Biochemistry and Biophysics Reports

journal homepage: www.elsevier.com/locate/bbrep

# Three sample-sparing techniques to estimate the molar absorption coefficient of luminescent dyes

Jeffrey M. Schaub, Quinn A. Best, Cheng Zhao, Richard A. Haack, Qiaoqiao Ruan *

*Applied Research and Technology, Core Diagnostics, Abbott Laboratories, 100 Abbott Park Road, Abbott Park, IL, 60064-6016, United States*

ARTICLE INFO

*Keywords:*
Molar absorption coefficient
Molar extinction coefficient
Absorbance
Mass spectrometry
Fluorescence correlation spectroscopy

ABSTRACT

Luminescent dyes are commonly modified to improve their solubility, permeability, or spectral properties. However, changing the chemical structure influences the absorption of light and thus the compound-specific molar absorption coefficient ($\varepsilon$), which also confounds the compound's concentration in solution. The accurate determination of the molar absorption coefficient of new luminescent molecules is labor intensive and challenging when a limited amount of material is available for testing. To address this problem, we developed three techniques combined with UV–Vis spectrophotometry to closely approximate the molar absorption coefficient of various light-emitting dyes. The first technique uses Electrospray Mass Spectrometry to obtain a high-resolution incorporation ratio of a dye-labeled protein. The second approach utilizes covalent linking of the unknown dye to a dye with a known absorption coefficient. In the third method, we used fluorescence correlation spectroscopy to determine the fluorophore concentration in solution. We test each method with well-characterized fluorescent dyes and an uncharacterized chemilumiphore. Each technique produced calculated absorption coefficients comparable to the published reference values, although each presented unique limitations that reduced accuracy under certain conditions. Nevertheless, the techniques could be incorporated into current compound evaluation workflows and require only a small amount of sample, two significant advantages over traditional methods for characterizing new luminescent compounds.

## 1. Introduction

Immunofluorescence as a research tool emerged in the 1940s, when fluorescein isothiocyanate was used to directly label antibodies [1,2]. In the following decades, other fluorescent dyes were developed and utilized for fluorescence measurements, including rhodamine, coumarin, and cyanine fluorophores [3,4]. These dyes serve as the structural backbone of many commonly used modern fluorophores, including the popular Alexa Fluor series dyes suited for biological applications. To meet the diversity of fluorescence needs, fluorophores continue to be extensively modified to improve characteristics such as solubility, membrane permeability, or spectral properties [5–7]. Each new fluorescent dye must be accurately characterized prior to its use.

The concentration of a dye in solution is calculated by Beer's Law, where the absorption of light is directly correlated to the concentration of the species, the path length of the measurement, and the compound-specific measure of light absorbance, its molar absorption coefficient ($\varepsilon$). Adding or removing functional groups from dyes changes the electron localization pattern and impacts how efficiently light is absorbed. Modification effects can be approximated by theoretical calculations with either computational and machine learning resources or by the Strickler-Berg relation if the quantum yield and fluorescence lifetime are known [8–11]. However, even small modifications cause shifts in the molar absorption coefficient [12]. For example, fluorescein has an absorption peak at 490 nm and absorption coefficient of around 80,000 $M^{-1}$ $cm^{-1}$ in a basic solution [13,14]. Switching the hydroxyl groups at the 3,6 position of the xanthene core with an amines yields rhodamine 110, which has a lower absorption coefficient of 76,000 $M^{-1}$ $cm^{-1}$ [15]. Addition of a carboxy moiety on the rhodamine 110 phenyl group at the 5′ position increases the absorption coefficient to 84,000 $M^{-1}$ $cm^{-1}$ [16]. Sulfonation of 5-carboxy-rhodamine 110 at positions 4,5 position generates the popular Alexa Fluor 488 dye and reduces the absorption coefficient to 73,000 $M^{-1}$ $cm^{-1}$ [17]. Removal of the 5′ carboxyl group and tertiary amide substitution at the 2′ carboxyl group creates ATTO 488 dye with a higher absorption coefficient of 90,000 $M^{-1}$ $cm^{-1}$ [18]. Thus, modification of these xanthene dyes alter the absorption coefficient upwards of 20 %. Similarly, modification of the 3,6 positions of tetramethylrhodamine with differently sized nitrogen-containing rings

* Corresponding author. AP-20, Abbott Laboratories, 100 Abbott Park Road, Abbott Park, IL, 60064-6016, United States.
*E-mail address:* qiaoqiao.ruan@abbott.com (Q. Ruan).

https://doi.org/10.1016/j.bbrep.2025.101971
Received 8 November 2024; Received in revised form 18 February 2025; Accepted 3 March 2025

changes the absorption coefficient from 0 to 40 % without a clear correlation on ring size [6]. In addition to fluorophores, other dyes such as chemiluminescent acridinium ester derivatives are modified to improve light yield, solubility, and other properties [19].

The development of new, brighter fluorophores with more efficient light yield requires accurate measurement of the absorption coefficient and precise dye concentrations in solution. For researchers and organic chemists developing new light-emitting dyes, absorbance cannot be used to quantify a compound without *a priori* determination of the molar absorption coefficient. Traditionally, the molar absorption coefficient of a new dye is determined by measuring the absorbance of a sample of known concentration. To ensure the accuracy of the solution concentration, the new dye's formula weight must then be calculated by performing elemental analysis to account for deviations from hydration states, residual solvent, impurities, etc. [20] This is especially important for novel dyes with unoptimized synthesis protocols. However, formula weight measurements are subject to experimental and random error, complicating the analysis of purity [21]. Additionally, the whole process requires significant sample preparation (~50 mg) and outsourcing the elemental analysis to third-party laboratories, which can be costly and time-consuming.

There is a need for low sample consumption methods that can accurately determine a new dye's absorption coefficient for quantification and light yield estimation, ideally, with accuracies within 20 % of the true value [22,23]. Here, we apply three independent techniques to approximate the concentration of light-emitting dyes and derive their absorption coefficients. We test well-characterized Alexa fluorophores as controls and further apply the techniques to estimate the absorption coefficient of an uncharacterized chemiluminophore (Carboxylpropyl-sulfopropyl acridinium, CPSP) compared to traditional methods. Importantly, these three techniques use a fraction of the amount of sample as traditional elemental analysis and can be integrated into current compound evaluation workflows to rapidly and accurately characterize new luminescent dyes.

## 2. Methods

### 2.1. Reagents

Alexa Fluor 405-N-hydroxysuccinimide (NHS) (Invitrogen, Carlsbad, CA; A30000), Alexa Fluor 488-NHS (Invitrogen, A20000), Alexa Fluor 555-NHS (Invitrogen, A20009), Alexa Fluor 647-NHS (Invitrogen, A37573), and CPSP-NHS (in-house, Abbott Laboratories, Abbott Park, IL) were used for either reacting with Cy5 (Lumiprobe, Cockeysville, MD; 43020) or labeling a recombinant antibody fragment (rFab, Abbott) for mass spectrometry. Alexa Fluor 405-Dibenzocyclooctyne (DBCO) (Click Chemistry Tools, Carlsbad, CA; 1310), Alexa Fluor 430-DBCO (Click Chemistry Tools, 1274), Alexa Fluor 488-DBCO (Click Chemistry Tools, 1278), Alexa Fluor 532-DBCO (Click Chemistry Tools, 1282), Alexa Fluor 546-DBCO (Click Chemistry Tools, 1286), Alexa Fluor 568-DBCO (Click Chemistry Tools, 1294), and Alexa Fluor 594-DBCO (Click Chemistry Tools, 1298) were used for control dyes for fluorescence correlation spectroscopy (FCS) measurements. Alexa Fluor 488-NHS (Invitrogen, A20000) was used as an FCS standard. All dyes were suspended in DMSO (Invitrogen, D12345) and diluted in phosphate-buffered saline (PBS) for absorbance measurements or a HEPES-buffered saline with EDTA and Surfactant P20 (HBS-EP, Cytiva, Marlborough, MA; BR100188) for FCS measurements. All Alexa Fluor dye absorption coefficients were obtained from the product website as measured in potassium phosphate buffer (pH 7) [17].

The absorption coefficient for CPSP was calculated using the traditional approach of elemental analysis and weighing as described in the Supplemental Methods. We performed triplicate measurements and plotted the absorbance compared to the CPSP concentration (Fig. S1). The measured absorption coefficient of CPSP was 15,000 ± 100 $M^{-1}$ $cm^{-1}$ at 369 nm. All absorption coefficients herein refer to the non-UV absorbance wavelength peak of the compound.

### 2.2. Absorbance and concentration determination

Sample absorption spectra were measured on a Cary 4000 spectrophotometer (Agilent, Santa Clara, CA) in 1 cm quartz cuvettes (Hellma, Müllheim, Germany). Dye concentrations were determined based on absorbance (Abs) using Beer's law in Equation (1).

$$Abs = \varepsilon * c * l \tag{1}$$

Where $\varepsilon$ is the molar absorption coefficient ($M^{-1}$ $cm^{-1}$), $c$ is the concentration of the sample (M), and $l$ is the path-length (cm) of the cuvette used in the measurement.

### 2.3. Electrospray mass spectrometry

A recombinant mouse monoclonal antibody fragment (rFab, Abbott) was produced in house (Fig. S2). NHS-dye constructs were freshly prepared in DMSO (Invitrogen, D12345) and were mixed with the rFab overnight at three different concentrations in 100 mM sodium bicarbonate buffer pH 8.3 at 4 °C. Unreacted dye was removed by 7K MWCO spin desalting columns (ThermoFisher, Waltham, MA; 89883) and the dye-labeled rFab was eluted into PBS pH 7.2. rFab-dye absorbances were measured in PBS prior to mass spectrometry. Additionally, dyes alone were diluted in PBS to measure the absorbance to calculate the correction factors for 280 nm absorbance as shown in Equation (2), where λ is the peak absorbance of the dye (Fig. S3).

$$CF_{280\ nm} = \frac{Abs_{280\ nm}}{Abs_{\lambda}} \tag{2}$$

rFab-Dye absorbance at 280 nm was corrected for the contribution of each dye in Equation (3).

$$Abs_{280\ nm\ corr.} = Abs_{280\ nm} - (Abs_{\lambda} * CF_{280\ nm}) \tag{3}$$

The rFab absorption coefficient was determined based on the mouse IgG $\varepsilon^{0.1\ \%}$ of 1.40 $(mg/mL)^{-1}$ $cm^{-1}$, which correlates to a molar absorption coefficient of 70,000 $M^{-1}$ $cm^{-1}$, based on the rFab molecular weight of 50,000 g $mol^{-1}$ (see Supplementary Information) [24]. The rFab concentration was estimated using the $Abs_{280\ nm\ corr.}$ value using Beer's Law.

The conjugated Fab samples were desalted using Amicon® Ultra-10 K filters (Millipore, Burlington, MA). Desalted samples were analyzed using a TripleTOF® 5600 mass spectrometer (Sciex, Toronto, ON, Canada) coupled to an Eksigent MicroLC 200 HPLC (Sciex) using a C18 OPTI-TRAP™ cartridges (Optimize Technologies Inc., Oregon City, OR). All data were deconvoluted with PEAKVIEW software (Sciex).

### 2.4. Cy5 conjugation

Cy5-linked dye synthesis is described in the Supplemental Information (Synthetic Schemes).

Dye absorbance spectra were measured in PBS, pH 7.2. The uncharacterized dye (Dye) was measured individually to identify the peak absorbance wavelength (λ). The absorbance spectrum of Cy5 was used to calculate the wavelength-specific Cy5 correction factor ($CF_{\lambda}$) relative to the absorbance peak at 650 nm using Equation (4).

$$CF_{\lambda} = \frac{Abs_{\lambda}\ Cy5}{Abs_{650\ nm}\ Cy5} \tag{4}$$

### 2.5. Fluorescence correlation spectroscopy (FCS)

FCS measurements were performed on an inverted microscope (Nikon, Melville, NY; TE300) with 780 nm two-photon excitation provided by a pulsed laser (Spectra-Physics, Milpitas, CA; Mai Tai HP) and emission light was collected on a fluorescence correlation spectrometer

(ISS, Alba A100, Champaign, IL). Resulting data was fit to the auto-correlation function in Equation (5) [25].

$$G(\tau) = G(0)*\left(1+\frac{8D\tau}{\omega^2}\right)^{-1} * \left(1+\frac{8D\tau}{z^2}\right)^{-\frac{1}{2}} \quad (5)$$

Where, $D$ is the diffusion constant and $G(0)$ is the extrapolated amplitude parameter. $G(0)$ is inversely correlated with fluorophore concentration. The point spread function of the excitation light was estimated by using a 20 nM stock of Alexa Fluor 488 and fixing the diffusion constant to 435 $\mu m^2\ s^{-1}$ to obtain ω (observation volume waist) and $z$ (observation volume length) [26].

## 3. Results

### 3.1. Technique 1: high-resolution incorporation ratio by mass spectrometry

One of the primary applications of fluorescent dyes is to label proteins for fluorescence microscopy or other light-emission applications. With the known absorption coefficients of the dye and the protein, along with the absorbance spectrum of the dye-labeled protein, we can determine the average incorporation ratio (IR). In Technique 1, we reversed this approach by determining the incorporation ratio of the dye-labeled protein by mass spectrometry, then back calculating the absorption coefficient from the absorbance spectrum and the protein and dye concentrations (Fig. 1a), as done previously for the measurement of DNA-labeled silver nanoclusters [27]. Previous work suggests that there is a linear correlation between mass spectrometry-determined incorporation ratio and solution absorption-based incorporation ratio [28].

We selected a protein to label—a recombinant antibody fragment (rFab)—that would ionize as a clean, single peak on mass spectrometry (Fig. S2). The rFab was then labeled with three concentrations of CPSP-NHS ester to test variable incorporation ratios. Unreacted dye was removed via size exclusion chromatography, and the absorbance spectra of the rFab-CPSP, as well as CPSP-NHS alone, were measured to determine the correction factor (CF) at 280 nm (Fig. 1b and Fig. S3b). The rFab-CPSP was ionized, and we observed distinct molecular weight peaks that correlated to the unlabeled rFab, as well as the rFab labeled with 1–5 CPSP molecules (Fig. 1b), each separated by an average of 568 ± 2 Da (Fig. S4). We calculated the average incorporation ratio by weighting the rFab peak intensities by the number of CPSP molecules attached, divided by the total sum of rFab peak intensities. Using the rFab-CPSP absorbance spectra, we calculated the concentration of rFab based on the corrected ultraviolet (280 nm) absorbance, and then estimated the CPSP concentration based on the average IR. Finally, using Beer's law, we approximated the absorption coefficient of CPSP to be 17,000 ± 2500 $M^{-1}\ cm^{-1}$ (Table S1). This estimation is close to the absorption coefficient of 15,000 $M^{-1}\ cm^{-1}$ determined by the traditional method (Fig. S1).

To confirm that Technique 1 worked for other dyes, we tested four fluorophores, Alexa Fluor 405, Alexa Fluor 488, Alexa Fluor 555, and

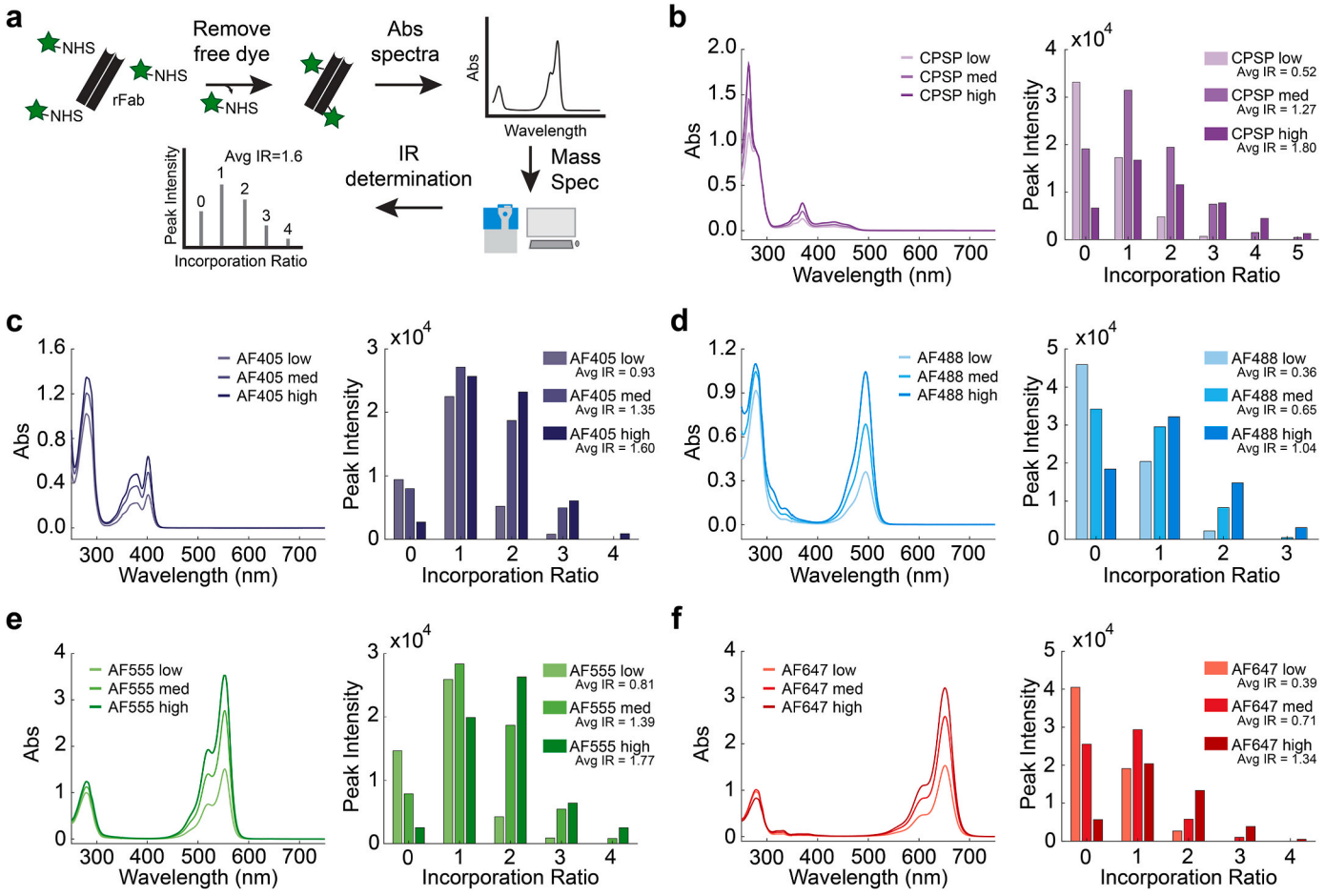


**Fig. 1. High-resolution incorporation ratio determination of absorption coefficients via electrospray mass spectrometry (Technique 1).** (a) Schematic of the workflow to label a rFab with amine-reactive (NHS) dye, with subsequent absorbance measurement and mass spectrometry. Absorbance spectrum (left) of three different rFab:dye ratios of (b) rFab-CPSP, (c) rFab-AF405, (d) rFab-AF488, (e) rFab-AF555, and (f) rFab-AF647 and the corresponding mass spectrometry-determined incorporation ratios (right). Average incorporation ratios (Avg IR) are noted.

Alexa Fluor 647, representing dyes with coumarin, rhodamine, and cyanine backbones with absorbances across the visible spectrum. We again labeled the rFab with three concentrations of each Alexa dye and measured the absorbance spectrums (Fig. 1c–f, Figs. S3c–f). The rFab-fluorophores incorporation ratios were measured via mass spectrometry. We measured between 1 and 4 incorporations of Alexa Fluor 405, Alexa Fluor 488, Alexa Fluor 555, and Alexa Fluor 647, separated by an average of 610 ± 0.3, 516 ± 0.6, 815 ± 0.4, and 841 ± 0.4 Da, respectively (Fig. 1c–f, Figure S5-8). Using the average incorporation ratio of Alexa Fluor 405, we calculated the absorption coefficient to be 29,000 ± 1800 $M^{-1}$ $cm^{-1}$, compared to the published reference of 35,000 $M^{-1}$ $cm^{-1}$ (Table S1). For Alexa Fluor 488, we measured the absorption coefficient to be 78,000 ± 2800 $M^{-1}$ $cm^{-1}$, in close agreement with the reference of 73,000 $M^{-1}$ $cm^{-1}$. Similar to Alexa Fluor 555, the measured absorption coefficient was 151,000 ± 4600 $M^{-1}$ $cm^{-1}$, comparable to the reference of 155,000 $M^{-1}$ $cm^{-1}$. Lastly, the absorption coefficient for Alexa Fluor 647 was estimated to be 268,000 ± 32,000 $M^{-1}$ $cm^{-1}$, nearly the same as the reference of 270,000 $M^{-1}$ $cm^{-1}$.

By labeling in triplicate, we were able to provide an average absorption coefficient. We did not observe a trend with higher labeling leading to an over- or underestimate in the absorption coefficient suggesting that ionization efficiency is similar across the samples. Overall, we were able to approximate the absorption coefficient of four fluorophores and one chemilumiphore within 20 % of the reference value. Thus, mass spectrometry can be used to estimate dye incorporation ratios and calculate the absorption coefficient of dyes with minimal sample consumption (less than 1 mg).

### 3.2. Technique 2: covalent linkage to Cy5

Here, we developed a method to tie the absorption coefficient of an unknown dye to a dye with a known absorption coefficient. The cyanine dye Cy5 has a strong absorbance peak centered around 650 nm with minimal absorbance below 550 nm (Fig. 2a). We reasoned that we could covalently link Cy5 to a dye of interest with near-UV to green absorbance. With the known absorption coefficient of Cy5, the absorption peak ratio of the linked compound could be used to provide a reasonable estimation of the absorption coefficient of the new compound. CPSP-NHS was reacted with piperazine (Pz) and subsequently purified before reaction with Cy5-NHS, to create Cy5-Pz-CPSP with the dyes linked in a 1:1 ratio (see Synthetic Schemes in the Supplemental Information) [29].

We measured the absorbance of CPSP alone, Cy5 alone, and the linked Cy5-Pz-CPSP construct on the spectrophotometer (Fig. 2a and b). We observed an additive effect in the spectrum for Cy5-Pz-CPSP (Fig. 2b). Using the Cy5 correction factor at 369 nm, we resolved the independent absorbance contribution of CPSP. Since the absorbance was normalized to the maximal Cy5 absorbance, we multiplied the fractional absorbance of the CPSP peak by the maximal absorption coefficient of Cy5 (250,000 $M^{-1}$ $cm^{-1}$) to obtain the absorption coefficient of CPSP. We therefore calculated the absorption coefficient of CPSP to be 14,000 ± 100 $M^{-1}$ $cm^{-1}$, which was close to our reference measurement of 15,000 $M^{-1}$ $cm^{-1}$ (Fig. S1). Using HPLC, Cy5-Pz-CPSP was measured to have a purity of 95.2 % at 641 nm, indicating that a negligible amount of Cy5 impurities were present in the synthesized and purified product (Fig. S9a, Table S2).

We performed the same synthesis with two additional dyes, Alexa

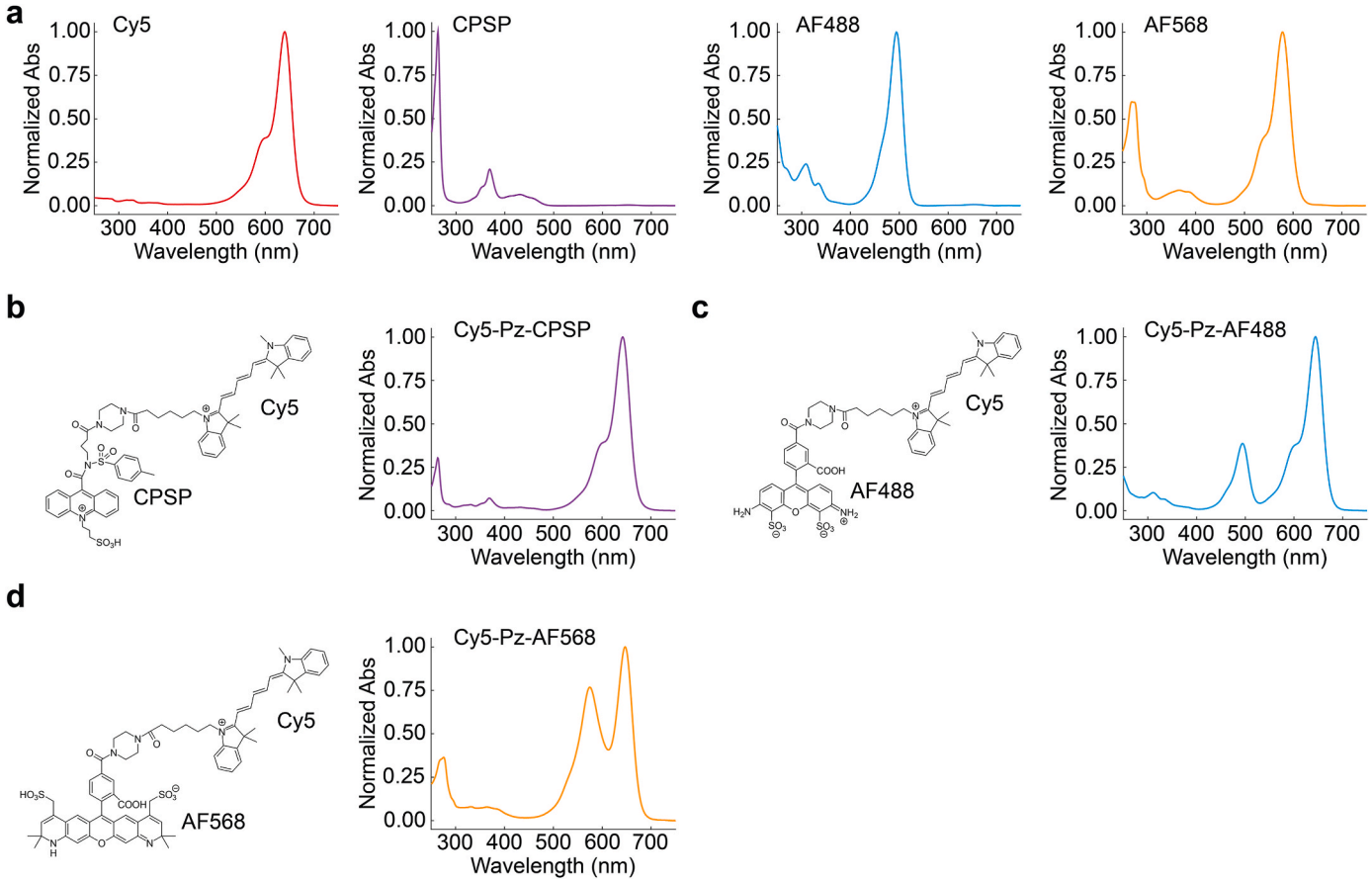


**Fig. 2. Cy5-linked dye compounds for absorption coefficient determination (Technique 2).** (a) Absorbance spectra of Cy5, CPSP, AF488, and AF568 in PBS. Structure (left) of (b) Cy5-Pz-CPSP, (c) Cy5-Pz-AF488, or (d) Cy5-Pz-AF568 and corresponding linked-dye absorbance spectra (right). Spectra are averages of three absorbance measurements.

Fluor 488 (Cy5-Pz-AF488) and Alexa Fluor 568 (Cy5-Pz-AF568). Similar to the CPSP construct, we observed the addition of the linked dye absorbance profiles to Cy5 (Fig. 2c and d). Alexa Fluor 488 and Alexa Fluor 568 have reference absorption coefficients of 73,000 and 88,000 $M^{-1}$ $cm^{-1}$, respectively; thus, we anticipated the absorbance peaks to be around 30 %–35 % of the Cy5 intensity. Instead, we observed that the Alexa Fluor 488 absorbance peak of compound 2 was 39 % and the Alexa Fluor 568 absorbance peak of compound 3 was 77 % of the Cy5 intensity (Table S2). After correction for the Cy5 absorbance at the linked wavelengths, we calculated the Alexa Fluor 488 and Alexa Fluor 568 absorption coefficients to be 93,000 ± 100 and 130,000 ± 200 $M^{-1}$ $cm^{-1}$, respectively. Error represents standard deviations from triplicate

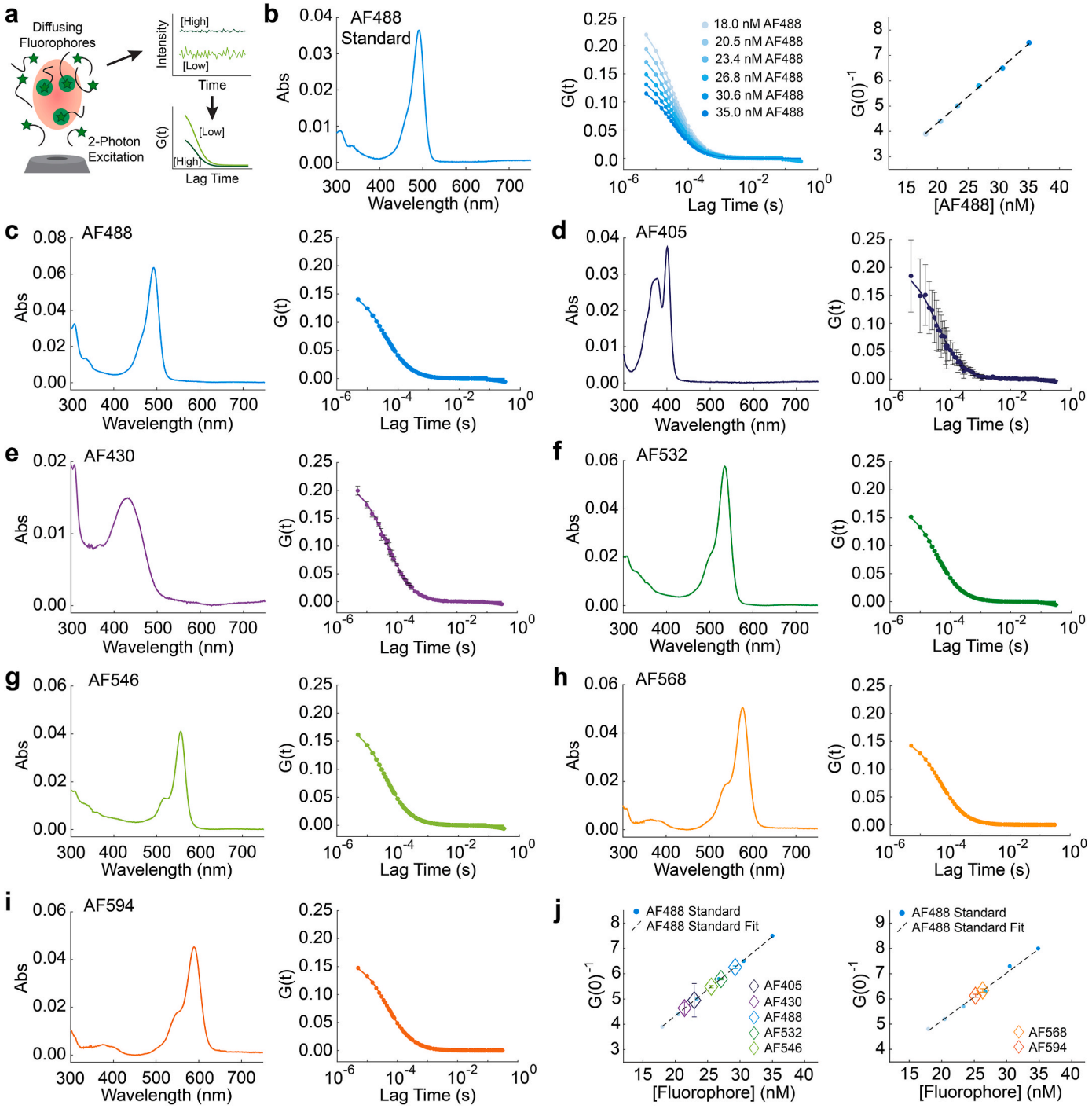


**Fig. 3. Fluorescence correlation spectroscopy (FCS) determination of fluorophore absorption coefficients (Technique 3).** (a) Schematic of 2-photon excitation fluorescence correlation spectroscopy (FCS). Lower concentrations of dye show larger deviations in fluorescence intensity due to diffusion than higher concentrations. Fitting the intensity data with an autocorrelation function shows differences in the G(t) based on dye concentration. (b) Absorbance spectra of AF488 to determine the stock concentration using the reference absorption coefficient of 73,000 $M^{-1}$ $cm^{-1}$ (left). Autocorrelation curves of six AF488 dilutions from 18 to 35 nM (middle). Corresponding linear fit of six AF488 dilutions and the $G(0)^{-1}$ to generate a standard curve (right). Solutions of (c) AF488, (d) AF405, (e) AF430, (f) AF532, (g) AF546, (h) AF568, and (i) AF594 with stock absorbance spectra (left) and corresponding diluted autocorrelation curve. (j) Mapping the $G(0)^{-1}$ values from (c) to (i) onto the AF488 standard curve to determine the fluorophore concentration in solution. Dyes measured at 25 mW (left) or 7.5 mW (right) laser intensity. The AF488 standards were measured on different days. Error bars represent standard deviation of three independent FCS measurements.

dilutions and absorption measurements from a single synthesis, suggesting accurate absorbance measurements but systematic deviation from the fluorophore-fluorophore construct. In both cases, these were large deviations from the expected values and Technique 2 was not a reliable method for deriving the absorption coefficient of these two fluorophores.

Previously, we reported a series of acridinium-linked fluorophores to achieve red-shifted chemiluminescence emission [23]. From this series, we selected a few compounds to see if the molar absorption coefficient of CPSP could be determined as performed for Cy5-Pz-CPSP. By measuring the absorbance spectra of Lucifer Yellow-Pz-CPSP, AF532-Pz-CPSP, and AF568-Pz-CPSP (Fig. S10), all three of these fluorophore-CPSP constructs accurately predicted the CPSP absorption coefficient (Table S2). From HPLC analysis, we confirmed that all the samples provided single peaks and were of high purity (Fig. S9). Therefore, we demonstrate reproducible absorption coefficient determination of CPSP using Technique 2 with a moderate sample consumption (around 5 mg).

### 3.3. Technique 3: fluorophore concentration determination by fluorescence correlation spectroscopy (FCS)

FCS measures the fluorescence signal fluctuation as fluorophores randomly diffuse in and out of a small illumination volume (Fig. 3a) [30]. The fluctuations in fluorescence intensity can be calculated by autocorrelation functions and the derived autocorrelation curve provides information on fluorophore concentration, size, and brightness [31]. Previous studies have used the well-defined illumination volume of FCS to calculate fluorophore concentration in solution, including for the molar absorption coefficient determination of quantum dots [32,33]. We posited that, using a fluorophore standard of known concentration, we would not need to determine the illumination volume which changes with laser power and excitation wavelength [34]. Instead, using the autocorrelation amplitude, $G(0)$, we can calculate the concentration of an unknown fluorophore without requiring the absorption coefficient.

We calibrated our system with Alexa Fluor 488 with a two-photon excitation wavelength of 780 nm. The Alexa Fluor 488 stock concentration was precisely measured by absorbance measurements on a spectrophotometer and then diluted over six concentrations in a narrow range of 35 to 18 nM (Fig. 3b). We observed the expected inverse relationship between concentration and autocorrelation curve amplitude $G(0)$. Plotting $G(0)^{-1}$ as a function of Alexa Fluor 488 concentration showed a linear relationship (Fig. 3b).

As an initial control, we prepared a second, independent stock of Alexa Fluor 488 dye and measured the absorbance spectra but did not use the absorption coefficient to calculate the concentration (Fig. 3c). Instead, we diluted the Alexa Fluor 488 dye until the $G(0)$ value fell within the range of our original Alexa Fluor 488 standard curve. Based on the $G(0)^{-1}$, we estimated the Alexa Fluor 488 concentration in solution to be 29.2 ± 0.2 nM. We then multiplied by the dilution factor to back-calculate the original Alexa Fluor 488 stock concentration. With our calculated concentration and original absorbance measurement, we used Beer's Law to estimate the absorption coefficient to be 71,000 ± 500 $M^{-1}$ $cm^{-1}$, which was nearly the Alexa Fluor 488 reference value of 73,000 $M^{-1}$ $cm^{-1}$ (Table S3).

To further test Technique 3, we generated stock solutions of a series of Alexa fluorophores, measured their absorbance spectra, and then diluted the dye stocks until the $G(0)$ fell within our Alexa Fluor 488 standard (Fig. 3d–i). The resulting $G(0)$ reciprocals were mapped onto the linear standard to calculate the dye concentrations (Fig. 3j). With our calculated concentrations and original absorbance measurements, we used Beer's Law to estimate the absorption coefficients. Alexa Fluor 405 was weakly excited; however, we were able to estimate the absorption coefficient to be 36,000 ± 4800 $M^{-1}$ $cm^{-1}$, comparable to the reference of 35,000 $M^{-1}$ $cm^{-1}$. Similar results were seen for Alexa Fluor 430, with an estimated absorption coefficient of 15,000 ± 800 $M^{-1}$ $cm^{-1}$, exactly matching the reference value of 15,000 $M^{-1}$ $cm^{-1}$. Technique 3 also performed well with dyes with higher reference absorption coefficients; both Alexa Fluor 532 ($\varepsilon$ = 82,000 $M^{-1}$ $cm^{-1}$) and Alexa Fluor 546 ($\varepsilon$ = 112,000 $M^{-1}$ $cm^{-1}$) had calculated values of 80,000 ± 400 $M^{-1}$ $cm^{-1}$ and 108,000 ± 1000 $M^{-1}$ $cm^{-1}$, respectively. The calculated absorption coefficients of Alexa Fluor 568 and Alexa Fluor 594 were 94,000 ± 1000 $M^{-1}$ $cm^{-1}$ and 90,000 ± 900 $M^{-1}$ $cm^{-1}$ compared to the reference values of 88,000 and 92,000 $M^{-1}$ $cm^{-1}$, respectively (Table S3). This technique requires accurate dilutions to properly calculate the original stock concentration. Across the samples tested, error estimates are quite low, from the average of three independent fluorophore dilutions. The largest error, Alexa Fluor 405, was also the weakest excited fluorophore. All dyes tested were within 10 % of their reference absorption coefficient value.

We noted that for Alexa Fluor 568 and Alexa Fluor 594, the data was poorly approximated with the autocorrelation function when measured at 25 mW laser intensity. We performed a power study to measure the $G(0)$ values of Alexa Fluor 488, Alexa Fluor 568, Alexa Fluor 594, and Alexa Fluor 647 (Fig. S11). While Alexa Fluor 488 showed stable autocorrelation regardless of laser intensity, we only saw the Alexa Fluor 568 and Alexa Fluor 594 autocorrelation stabilize below 10 mW. We therefore measured the Alexa Fluor 488 standard, Alexa Fluor 568, and Alexa Fluor 594 at 7.5 mW intensity to derive the dye concentrations (Fig. 3j, right). We did not observe the $G(0)$ of Alexa Fluor 647 stabilize and the absorption coefficient was therefore not determined (Fig. S11). Additionally, CPSP is not effectively excited and could not be measured using this method. Nevertheless, FCS appeared to be a useful tool to estimate the concentration of a broad spectral range of fluorophores directly in solution; the concentration can be then used to accurately calculate absorption coefficients with negligible fluorophore consumption (less than 1 mg).

## 4. Conclusion

We developed and tested three techniques to quantify molar absorption coefficients, which could be introduced into compound evaluation workflows for a rapid, sample-conserving screen prior to more costly and labor-intensive traditional elemental analysis of new luminescent dyes. Utilizing these three techniques provided mixed success, with the mass spectrometry and FCS providing reliable results for the fluorophore measurements and, the CPSP measurements were most consistent with the mass spectrometry and linked-dye measurements. Overall, 16 out of 18 experiments estimated the dye's molar absorption coefficient within 20 % of the reference (Table 1). However, each method presented some inherent limitations and required access to specialized equipment (Table 2).

In the first technique, a recombinant antibody fragment (rFab) is labeled with various concentrations of dyes and mass spectrometry is used to determine the incorporation ratio. We then calculate the absorption coefficient by extrapolating the dye concentration from the rFab absorbance and average incorporation ratio. Mass spectrometry analysis requires specific technical expertise, and the dye requires functionalization to conjugate to a protein. Heterogenous post-translational modifications of proteins could introduce challenges to calculate incorporation ratio accurately. Therefore, we always evaluate the protein before labeling to determine the molecule weight peak of IR = 0. We therefore recommend testing the unlabeled protein first to determine peak cleanliness. The major limitation with mass spectrometry-based absorption coefficient determination is the assumption that the dye-labeled protein ionizes at the same efficiency as the unlabeled protein. We performed an experiment with a Cy5-labeled rFab that poorly estimated the absorption coefficient of Cy5 (Fig. S12). In this example, the incorporation ratio based on mass spectrometry was lower than expected compared to the absorbance-based incorporation ratio, thus overapproximating the Cy5 absorption coefficient. We attribute this to the lower ionization efficiency of the Cy5-labeled species compared to the unlabeled protein, which underestimated the dye

**Table 1**
Comparison of reference molar absorption coefficients to calculated values via three described techniques.

| Method | Dye | Reference $\varepsilon$ | Calculated $\varepsilon$ | Difference (%) |
|---|---|---|---|---|
| Mass Spec. | CPSP | 15,000 | 17,000 ± 2,500 | 13.3 |
| Mass Spec. | Alexa Fluor 405 | 35,000 | 29,000 ± 1,800 | 17.1 |
| Mass Spec. | Alexa Fluor 488 | 73,000 | 78,000 ± 2,800 | 6.8 |
| Mass Spec. | Alexa Fluor 555 | 155,000 | 151,000 ± 4,600 | 2.6 |
| Mass Spec. | Alexa Fluor 647 | 270,000 | 268,000 ± 32,000 | 0.7 |
| Linked-Dye | CPSP | 15,000 | 14,000 ± 100 | 6.7 |
| Linked-Dye | Alexa Fluor 488 | 73,000 | 93,000 ± 100 | 27.4 |
| Linked-Dye | Alexa Fluor 568 | 88,000 | 130,000 ± 200 | 48.9 |
| Linked-Dye | CPSP | 15,000 | 17,000 ± 100 | 13.3 |
| Linked-Dye | CPSP | 15,000 | 16,000 ± 100 | 6.7 |
| Linked-Dye | CPSP | 15,000 | 16,000 ± 100 | 6.7 |
| FCS | Alexa Fluor 405 | 35,000 | 36,000 ± 4,800 | 2.9 |
| FCS | Alexa Fluor 430 | 15,000 | 15,000 ± 800 | 0.0 |
| FCS | Alexa Fluor 488 | 73,000 | 71,000 ± 500 | 2.7 |
| FCS | Alexa Fluor 532 | 81,000 | 82,000 ± 400 | 1.2 |
| FCS | Alexa Fluor 546 | 112,000 | 108,000 ± 1,000 | 3.6 |
| FCS | Alexa Fluor 568 | 88,000 | 94,000 ± 1,000 | 6.8 |
| FCS | Alexa Fluor 594 | 92,000 | 90,000 ± 900 | 2.2 |

concentration. In comparison, the absorption coefficient of Alexa Fluor 647, a sulfonated version of Cy5, was correctly estimated using this technique. Therefore, this mass spectrometry -based approach may be more advantageous for evaluation of charged dyes.

The second technique involves covalently linking a dye of interest to a dye with a known absorption coefficient at 1:1 ratio. Linking the dye of interest to a known dye is a straightforward process for an organic chemistry lab synthesizing compounds; however, the process requires dye functionalization and a nontrivial amount of sample (~5 mg). Of the three techniques tested, this method provided the least accurate results for the control Alexa Fluor dyes. We observed that the accuracy of this technique decreased the closer the linked dye absorbance spectra was to that of the companion dye, Cy5. That is, the spectra overlap of the linked Alexa Fluor dye and the Cy5 dye decreased the accuracy of the estimated absorption coefficient. This effect may be attributed to the physical proximity of the linked dyes, with electron withdrawing or donating effects such as static quenching causing distortion of the absorption spectrum [35]. Introduction of a longer linker may mitigate this effect. Notably, we were able to closely approximate the absorption coefficient with the attachment of the weakly fluorescent CPSP to Cy5, Lucifer Yellow, Alexa Fluor 532 and 568, possibly due to the low absorption coefficient of the dye, or the weakness of the fluorescence dye properties, which may reduce dye-to-dye interactions. Future renditions of this experiment could involve alternative linkers between the dye of interest and the companion fluorophore, such as reducible, enzyme-cleavable, or meltable (ie, DNA oligo) linked dyes. In this way, the dye of interest and known fluorophore are assembled at a 1:1 ratio and then separated from each other to reduce dye-dye interactions and improve the reliability of the absorption coefficient measurement.

The third technique utilized two-photon fluorescence correlation spectroscopy (FCS) to build a correlation between the $G(0)$ value and fluorophore concentration with the well-characterized fluorophore Alexa Fluor 488, and then applied the correlation to the unknown fluorophore to derive its concentration. The FCS approach does not require additional preparation of the fluorophore and material consumption is negligible; however, it is only applicable to fluorophores and requires specialized instrumentation. In our study, we found that the autocorrelation curve of individual fluorophores is sensitive to the laser power used in the measurement. It is therefore essential to conduct a power study of each fluorophore to ensure the $G(0)$ is independent of the laser power. We anticipate that this method could be of use when modifying a fluorophore, where the parental dye serves as the autocorrelation standard to measure the concentration of each derivative dye. We used a single excitation wavelength at a single power level to maintain the fluorescence illumination volume across all measurements. We showed that the method is independent from excitation efficiency, emission wavelength, emission intensity, and diffusion coefficient; the fluctuations in fluorescence intensity are thus dependent only on the dye concentration. We pursued two-photon, instead of one-photon, FCS for two reasons. First, we found that the triplet state of the one-photon system obscures the correlation curve, it requires more careful analysis to account for the triplet state. Second, using a single excitation wavelength in the two-photon system at 780 nm, we were able to excite a broad range of fluorophores from Alexa Fluor 405 to Alexa Fluor 594. Similar one-photon excitation would require three laser lines and three fluorophore standards to achieve the same measurements. In practice, we found it is more straightforward to use two-photon as compared to one-photon excitation [36]. As an alternative to FCS, previous studies have used absorption saturation spectroscopy to determine absorption coefficients of fluorophores [37,38]. However, this technique also requires specific equipment for broad excitation intensities to saturate fluorophore ground state absorbance [37].

**Table 2**
Comparison of the traditional method and three new techniques for estimation of absorption coefficients of luminescent dyes.

| | Traditional: Elemental analysis/ weighing | Technique 1: Mass spectrometry | Technique 2: Linked dyes | Technique 3: Two-photon FCS |
|---|---|---|---|---|
| Sample requirement | ~50 mg | <1 mg | ~5 mg | <1 mg |
| Specialized equipment requirements | Analytical balance, Spectrophotometer, Outsourcing for elemental analysis | Mass spectrometer, Spectrophotometer | High-pressure liquid chromatography (HPLC), Spectrophotometer | FCS system, Spectrophotometer |
| Method requirements | – | Dye covalently attached to carrier protein and free dye removed | Target compound linked to dye at 1:1 ratio with high purity | – |
| Reagent requirements/ modifications | – | Functionalized dye (NHS, maleimide, etc.) | Functionalized dye (NHS, maleimide, etc.) | Dye must be fluorescent with two-photon excitation |
| Method limitations | Without performing elemental analysis, can lead to inaccurate concentration measurements | Differential ionization efficiency reduces accuracy (e.g. Cy5) | Overlap in absorption spectra reduces accuracy (e.g. Cy5-Pz-AF568) | Weak fluorescence (e.g. CPSP) or low two-photon absorption cross-section (e.g. Cy5) |

It is important to note the limitations we encountered in calculating the absorption coefficients using these techniques. As we observed with Alexa Fluor 488 and 568 in the linked compound experiment, Cy5 in the mass spectrometry measurement, and Alexa Fluor 647 in the FCS measurements, absorption coefficient estimations were inaccurate. However, these methods offer an approach to screening new luminescent dyes without intensive sample consumption and could be incorporated as complementary methods into traditional workflows to identify candidate compounds for validation by multiple methods.

## CRediT authorship contribution statement

**Jeffrey M. Schaub:** Writing – review & editing, Writing – original draft, Visualization, Methodology, Investigation, Formal analysis, Conceptualization. **Quinn A. Best:** Writing – review & editing, Methodology, Investigation, Formal analysis, Conceptualization. **Cheng Zhao:** Writing – review & editing, Methodology, Investigation, Formal analysis, Conceptualization. **Richard A. Haack:** Writing – review & editing, Methodology, Conceptualization. **Qiaoqiao Ruan:** Writing – review & editing, Methodology, Conceptualization.

## Funding

Abbott Laboratories provided all operating funds. No external funding sources were used in this study.

## Declaration of competing interest

The authors declare that they have no known competing financial interests or personal relationships that could have appeared to influence the work reported in this paper.

## Acknowledgements

We are thankful to our Abbott colleagues for providing reagents used in this study. We are also thankful to Bin Wu, PhD, for helpful discussions on FCS and the responses of dyes to laser intensity and to Stacey Tobin, PhD, for editorial support in the preparation of the manuscript.

## Appendix A. Supplementary data

Supplementary data to this article can be found online at https://doi.org/10.1016/j.bbrep.2025.101971.

## Data availability

Data will be made available on request

## References

[1] A.H. Coons, H.J. Creech, R.N. Jones, Immunological properties of an antibody containing a fluorescent group, PSEBM (Proc. Soc. Exp. Biol. Med.) 47 (1941) 200–202.
[2] A.H. Coons, H.J. Creech, R.N. Jones, E. Berliner, The demonstration of pneumococcal antigen in tissues by the use of fluorescent Antibody1, J. Immunol. 45 (1942) 159–170.
[3] L.D. Lavis, Teaching old dyes new tricks: biological probes built from fluoresceins and rhodamines, Annu. Rev. Biochem. 86 (2017) 825–843.
[4] J. Chan, S.C. Dodani, C.J. Chang, Reaction-based small-molecule fluorescent probes for chemoselective bioimaging, Nat. Chem. 4 (2012) 973–984.
[5] N. Panchuk-Voloshina, R.P. Haugland, J. Bishop-Stewart, M.K. Bhalgat, P. J. Millard, F. Mao, W.Y. Leung, R.P. Haugland, Alexa dyes, a series of new fluorescent dyes that yield exceptionally bright, photostable conjugates, J. Histochem. Cytochem. : official journal of the Histochemistry Society 47 (1999) 1179–1188.
[6] J.B. Grimm, B.P. English, J. Chen, J.P. Slaughter, Z. Zhang, A. Revyakin, R. Patel, J. J. Macklin, D. Normanno, R.H. Singer, T. Lionnet, L.D. Lavis, A general method to improve fluorophores for live-cell and single-molecule microscopy, Nat. Methods 12 (2015) 244–250, 243 pp. following 250.
[7] P.J. Macdonald, S. Gayda, R.A. Haack, Q. Ruan, R.J. Himmelsbach, S.Y. Tetin, Rhodamine-derived fluorescent dye with inherent blinking behavior for super-resolution imaging, Anal. Chem. 90 (2018) 9165–9173.
[8] R. Mamede, F. Pereira, J. Aires-de-Sousa, Machine learning prediction of UV-Vis spectra features of organic compounds related to photoreactive potential, Sci. Rep. 11 (2021) 23720.
[9] J.F. Joung, M. Han, J. Hwang, M. Jeong, D.H. Choi, S. Park, Deep learning optical spectroscopy based on experimental database: potential applications to molecular design, JACS Au 1 (2021) 427–438.
[10] J. Yan, X. Rodríguez-Martínez, D. Pearce, H. Douglas, D. Bili, M. Azzouzi, F. Eisner, A. Virbule, E. Rezasoltani, V. Belova, B. Dörling, S. Few, A.A. Szumska, X. Hou, G. Zhang, H.L. Yip, M. Campoy-Quiles, J. Nelson, Identifying structure-absorption relationships and predicting absorption strength of non-fullerene acceptors for organic photovoltaics, Energy Environ. Sci. 15 (2022) 2958–2973.
[11] S.J. Strickler, R.A. Berg, Relationship between absorption intensity and fluorescence lifetime of molecules, J. Chem. Phys. 37 (1962) 814–822.
[12] J.V. Jun, D.M. Chenoweth, E.J. Petersson, Rational design of small molecule fluorescent probes for biological applications, Org. Biomol. Chem. 18 (2020) 5747–5763.
[13] A. Baeyer, Ueber eine neue Klasse von Farbstoffen, Ber. Dtsch. Chem. Ges. 4 (1871) 555–558.
[14] L.D. Lavis, T.J. Rutkoski, R.T. Raines, Tuning the pK(a) of fluorescein to optimize binding assays, Anal. Chem. 79 (2007) 6775–6782.
[15] J.B. Grimm, A.J. Sung, W.R. Legant, P. Hulamm, S.M. Matlosz, E. Betzig, L.D. Lavis, Carbofluoresceins and carborhodamines as scaffolds for high-contrast fluorogenic probes, ACS Chem. Biol. 8 (2013) 1303–1310.
[16] J.B. Grimm, L.D. Lavis, Caveat fluorophore: an insiders' guide to small-molecule fluorescent labels, Nat. Methods 19 (2022) 149–158.
[17] The Alexa Fluor Dye Series—Note 1.1.
[18] Product Information: ATTO 488, 2022.
[19] A. Natrajan, D. Sharpe, Synthesis and properties of differently charged chemiluminescent acridinium ester labels, Org. Biomol. Chem. 11 (2013) 1026–1039.
[20] W. Kandioller, J. Theiner, B.K. Keppler, C.R. Kowol, Elemental analysis: an important purity control but prone to manipulations, Inorg. Chem. Front. 9 (2022) 412–416.
[21] R.E.H. Kuveke, L. Barwise, Y. van Ingen, K. Vashisth, N. Roberts, S.S. Chitnis, J. L. Dutton, C.D. Martin, R.L. Melen, An international study evaluating elemental analysis, ACS Cent. Sci. 8 (2022) 855–863.
[22] A.A. Tikhomirova, K.M. Swift, R.A. Haack, P.J. Macdonald, S.J. Hershberger, S. Y. Tetin, Acridone and acridinium constructs with red-shifted emission, Methods Appl. Fluoresc. 9 (2021) 025006.
[23] Q.A. Best, R.A. Haack, K.M. Swift, B.M. Bax, S.Y. Tetin, S.J. Hershberger, A rainbow of acridinium chemiluminescence, Luminescence : the journal of biological and chemical luminescence 36 (2021) 1097–1106.
[24] Using a NanoDrop™ to Measure Antibody Concentration, Vector Laboratories.
[25] T.L. Hazlett, Q. Ruan, S.Y. Tetin, Application of fluorescence correlation spectroscopy to hapten-antibody binding, Methods Mol. Biol. 305 (2005) 415–438.
[26] Z. Petrásek, P. Schwille, Precise measurement of diffusion coefficients using scanning fluorescence correlation spectroscopy, Biophys. J. 94 (2008) 1437–1448.
[27] G. Romolini, C. Cerretani, V. Rück, M.B. Liisberg, C.B. Mollerup, T. Vosch, Analytical method for the determination of the absorption coefficient of DNA-stabilized silver nanoclusters, Nanoscale 16 (2024) 12559–12566.
[28] Q. Ruan, C. Zhao, C.S. Ramsay, S.Y. Tetin, Characterization of fluorescently labeled protein with electrospray ionization-MS and fluorescence spectroscopy: how random is random labeling? Anal. Chem. 90 (2018) 9695–9699.
[29] R.A. Haack, S.J. Hershberger, Q.A. Best, K.M. Swift, S.Y. Tetin, Chemoselective reaction of bifunctional carboxysulfonic acid systems: preparation of useful intermediates for chemiluminescent, fluorescent and UV absorbing bifunctional linkers, Tetrahedron Lett. 61 (2020).
[30] L. Yu, Y. Lei, Y. Ma, M. Liu, J. Zheng, D. Dan, P. Gao, A comprehensive review of fluorescence correlation spectroscopy, Frontiers in Physics 9 (2021).
[31] N.L. Thompson, A.M. Lieto, N.W. Allen, Recent advances in fluorescence correlation spectroscopy, Curr. Opin. Struct. Biol. 12 (2002) 634–641.
[32] C. Dong, J. Ren, Measurements for molar extinction coefficients of aqueous quantum dots, Analyst 135 (2010) 1395–1399.
[33] M. Eigen, R. Rigler, Sorting single molecules: application to diagnostics and evolutionary biotechnology, Proc. Natl. Acad. Sci. U. S. A 91 (1994) 5740–5747.
[34] S.T. Hess, W.W. Webb, Focal volume optics and experimental artifacts in confocal fluorescence correlation spectroscopy, Biophys. J. 83 (2002) 2300–2317.
[35] J. Lakowicz, Principles of Fluorescence Spectroscopy, 1 ed., Springer, 1983.
[36] P.T. So, C.Y. Dong, B.R. Masters, K.M. Berland, Two-photon excitation fluorescence microscopy, Annu. Rev. Biomed. Eng. 2 (2000) 399–429.
[37] M.-M. Sildoja, J. Pahapill, C.W. Stark, A.K. Rebane, A.C. Peacock, G. Tissoni, J. M. Dudley, B. Stiller, Determining molar extinction coefficient by high-accuracy optical saturation measurements, in: Nonlinear Optics and its Applications 2024, 2024.
[38] I. Volkov, T. Sych, P. Serdobintsev, Z. Reveguk, A. Kononov, Fluorescence saturation spectroscopy in probing electronically excited states of silver nanoclusters, J. Lumin. 172 (2016) 175–179.